

# Contact Compliance Visuo-Proprioceptive Policy for Contact-Rich Manipulation with Cost-Efficient Haptic Hand-Arm Teleoperation System

Bo Zhou\*, Ruixuan Jiao\*, Yi Li\*, Fang Fang and Fu Chen

**Abstract**—Learning robot manipulation skills in real-world environments is extremely challenging. Robots learning manipulation skills in real-world environments is extremely challenging. Recent research on imitation learning and visuomotor policies has significantly enhanced the ability of robots to perform manipulation tasks. In this paper, we propose Admit Policy, a visuo-proprioceptive imitation learning framework with force compliance, designed to reduce contact force fluctuations during robot execution of contact-rich manipulation tasks. This framework also includes a hand-arm teleoperation system with vibrotactile feedback for efficient data collection. Our framework utilizes RGB images, robot joint positions, and contact forces as observations and leverages a consistency-constrained teacher-student probabilistic diffusion model to generate future trajectories for end-effector positions and contact forces. An admittance model is then employed to track these trajectories, enabling effective force-position control across various tasks. We validated our framework on five challenging contact-rich manipulation tasks. Among these tasks, while improving success rates, our approach most significantly reduced the mean contact force required to complete the tasks by up to 53.92% and decreased the standard deviation of contact force fluctuations by 76.51% compared to imitation learning algorithms without dynamic contact force prediction and tracking.

**Index Terms**—Imitation Learning, Contact-Rich Manipulation, Dexterous Teleoperation, Force Control.

## I. INTRODUCTION

THE vision of robots performing daily tasks for humans holds great promise. These tasks can be broken down into actions such as grasping, pushing, pulling, twisting, rubbing, turning, and scratching. Many of these actions involves extensive contact with tools or the environment, requiring precise force adjustment during the interaction process [1]–[4]. Current studies employ advanced imitation learning policy enabling robots to learn autonomous manipulation policies from demonstration trajectories and visual data, thereby developing a certain level of environmental understanding and task planning capabilities [5]–[7].

Current methods enable robots to learn autonomous manipulation policies from human demonstration trajectories and images through advanced imitation learning techniques, thereby developing a certain level of environmental understanding and

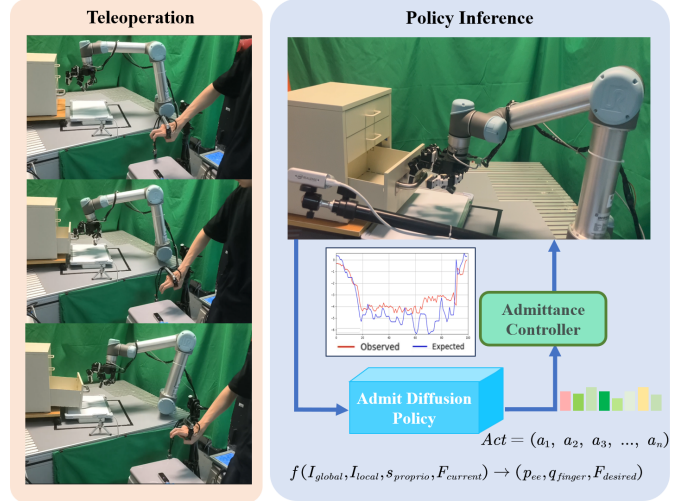


Fig. 1. Overview of teleoperation opening a drawer and performing visuo-proprioceptive policy inference.

task planning abilities. However, when applied to contact-rich manipulation tasks and interactions, these policies, which rely on trajectories and images, lack sensitivity to small motion errors. For robots using rigid position control in their joints, such minor motion errors can cause variations in the contact force of the end-effector during interaction with the environment or tools. These variations in contact force can lead to failures in tasks or even emergency stops due to collisions, increasing the difficulty of validating robotic policies.

Learning manipulation skills through imitation learning requires high-quality and sufficient demonstration data, rising a demand for an efficient teleoperation system during data collection. For hand-arm dexterous manipulation systems in teleoperation, tasks like identifying the wrist’s spatial pose and performing gesture remapping are necessary [8]–[10]. Teleoperation tasks can be accomplished by using either a monocular camera or Virtual Reality (VR) motion capture equipment. However, monocular cameras suffer from low accuracy, particularly in continuous recognition of wrist rotation, while VR and motion capture devices are often expensive or difficult to deploy. [11]–[14].

To effectively tackle these two challenges, we propose a new framework for imitation learning in contact-rich manipulation tasks, consisting of a series of innovative approaches. First, We utilized a binocular fisheye camera running a visual odometry program to capture the wrist’s spatial pose and employed a depth camera to reconstruct gestures for joint angle remapping

Bo Zhou, Ruixuan Jiao, Yi Li contributed equally to this work. Corresponding author: Bo Zhou.

All the authors are with the School of Automation, Southeast University, Nanjing 210096, P. R. China (emails: zhoubo@seu.edu.cn; 220232086@seu.edu.cn; 220221974@seu.edu.cn; ffang@seu.edu.cn; 220232052@seu.edu.cn)

of the multi-finger hand. This approach balances the cost and accuracy of teleoperation. Second, Force/Torque sensor data is introduced in the process of policy training and inference, enabling closed-loop control of the contact forces on the end effector by adjusting joint positions. This approach helps mitigate the risks of operational failure and emergency stops due to collisions [2]. We employ the admittance controller [4] as the robot’s low-level controller, which accepts the force-position trajectories planned by the policy. This setup ensures that the end effector can achieve both motion tracking and disturbance rejection in free space, as well as appropriate compliant dynamic behavior during interactions. Third, we distill the diffusion policy network to enable one-step denoising process. Integrating force control within the imitation learning paradigm imposes high demands on the real-time performance of policy inference. The continuity of inference results can be improved through interpolation, while distilling the policy network can reduce inference time. A schematic diagram of the entire framework as deployed in a real-world task is shown in Fig. 1.

The main contributions of this paper are as follows:

- 1) We developed a cost-effective, precise and easy-to-deploy hand-arm teleoperation system, with the entire system cost reduced to 300\$. In the evaluation experiment on teleoperation system, our system achieved efficiency and accuracy comparable to state-of-the-art methods.
- 2) We proposed a distilled visuo-proprioceptive policy for imitation learning, termed the Admit Policy, which serves as a high-level planner capable of estimating dynamic contact forces to perform complex manipulations that cannot be achieved with constant-force control.
- 3) We employ an admittance controller as the robot’s low-level controller to track the dynamically varying force-position actions predicted by the policy. This approach improves operational safety while minimizing overall contact force magnitude and fluctuations during manipulation, achieving efficient contact-rich operations with an average reduction in contact force of 53

This paper demonstrates the effectiveness of the teleoperation system and the visuo-proprioceptive imitation learning method in various contact-rich manipulation tasks. The teleoperation system enables efficient data collection, while the imitation learning method reduces contact force magnitude and significantly minimizes force fluctuation variance.

## II. RELATED WORKS

### A. Dexterous Teleoperation

In certain dexterous manipulation scenarios, industrial robot teach pendants often face difficulties in managing complex task environments and dynamic task requirements. Recent advancements in sensor technology have led to increased efforts toward enabling dexterous robot teleoperation by capturing human motion through various sensors and corresponding algorithms.

VR devices from video games can capture hand movements, and this capability has been applied to robot control.

For instance, [1], [4] and [15], [16] used VR devices to teleoperate the PR2 robot. The handheld controller captures the hand’s position and pose in real-time, while the user’s head-mounted display enhances reality, placing the human and robot in the same observational space. These methods with VR devices tend to be costly. [17] use Inertial Measurement Unit (IMU) and depth camera to capture human motion for robot control. [18]–[20] used tools like MediaPipe to predict hand pose and posture from image streams, controlling the robot’s end-effector and dexterous hand posture. This approach was successfully deployed on various robot platforms, such as UR5, Kuka, and Xarm. These monocular vision-based methods have delays and inaccuracies in estimating wrist poses and hand joint positions. Some researchers have designed specific master-slave control mechanisms for robot arm drag teaching [4], [8] [5], [21]. Other researchers focused on portability [6], [22]. They designed handheld grippers similar to robot grippers and used a GoPro camera running Visual-Inertial Odometry (VIO) algorithm to record the operator’s hand posture, remapping it to the robot’s end-effector posture. This approach completed tasks like washing dishes and folding clothes. These methods are difficult to adapt to multi-fingered hands. Each of these three approaches has limitations. Our method balances cost and effectiveness, maintaining wrist operation stability at a low cost, enabling hand pose control, and incorporating force feedback functionality.

### B. Robot Learning from Demonstrations

Learning directly from human demonstrations is an effective way to equip robots with various manipulation policies. The concept of behavioral cloning has been widely applied in this context [5], [23]–[29]. Researches have approached robot action prediction by framing it as a time series problem, employing transformer-based networks to enhance the accuracy of predictions. One study [5] used a transformer to predict an entire sequence of future actions, thereby reducing the impact of cumulative errors on robot decision-making and enabling the learning of various manipulation policies in high-dimensional action spaces on a dual-arm platform.

To address issues such as single-action prediction and the high-dimensionality of action spaces, one study [24] introduced probabilistic diffusion models into robot action prediction, enhancing the robustness of the algorithm. Additionally, to reduce the computational cost of high-dimensional continuous control, the study predicted the robot’s actions for the next 8 steps, thereby lowering computational demands. [25] applied diffusion models to goal-oriented navigation problems, predicting the robot’s movement direction based on the target scene and current observations. Furthermore, [30] have explored encoding human instructions using pre-trained text or visual encoders, embedding the encoded information into visual representations through Feature-wise Linear Modulation (FiLM), thereby enabling robots to perform multiple tasks simultaneously. Another study [31] concentrated on the aspect of force interaction within imitation learning. This study sought to enhance the robot’s performance in tasks involving intricate force interactions by employing compliant control strategies.

Our approach leverages the advantages of diffusion models in fitting high-dimensional action distributions. We designed a network capable of accurately fitting various distinct actions while simultaneously predicting the robot’s end-effector pose, hand joint movements, and contact forces. These predicted contact forces are then used to correct kinematic errors in real-world tasks, thereby achieving force compliance in complex contact operations. To mitigate the control latency caused by the slow inference speed of diffusion models, we adopted the concept of student-teacher distillation [32], enabling the model to perform single-step diffusion for action prediction, thereby providing better preconditions for responsive admittance control.

### C. Force Control in Learning-based Manipulation

Interactive force control methods are widely employed in manipulation tasks, as discussed in [2], [4], [33], [34]. In contact-rich environments, the inherent uncertainties often lead to challenges with position-based control strategies, which may not effectively prevent joint and structural damage during tasks requiring significant contact forces. To address this, direct and indirect force control strategies, typically incorporating external sensors, offer precise regulation of forces through motion control. Among the commonly utilized approaches are impedance control [35] and admittance control [3], both of which model the robotic arm as an adjustable mass-spring-damper system, thereby enabling dynamic adaptation of contact forces.

Impedance and admittance control techniques have been integrated into learning-based manipulation tasks. For instance, [36] employed Proportional-Derivative (PD) and admittance control methods to achieve closed-loop control of contact forces during both training and inference phases in robotic reinforcement learning, while simultaneously adjusting the end-effector trajectory. In a separate study, [31] utilized a prior knowledge base to predict contact forces and end-effector poses, with an admittance-based Whole-Body Control (WBC) system being implemented to execute these predictions. Kamijo et al. [37] proposed the Comp-ACT method, which integrates end-effector pose and six-dimensional force sensor data into an imitation learning framework to predict the robot’s end-effector pose and the stiffness parameters for the admittance controller. However, this method relies on a manually tuned constant goal wrench during teleoperation and task execution, necessitating stiffness adjustments to accommodate varying desired contact forces.

Variable stiffness constant-force control is often inadequate for complex dexterous manipulation tasks due to the numerous contact states involved and the frequent transitions between these states. Our approach surpasses the Comp-ACT methodology by estimating dynamic contact forces rather than predicting admittance controller parameters. The desired force-position trajectory is interpolated over predicted time steps, while a high-frequency admittance controller dynamically adjusts the motion based on real-time contact force variations, enhancing the robot’s ability to handle complex, contact-rich tasks.

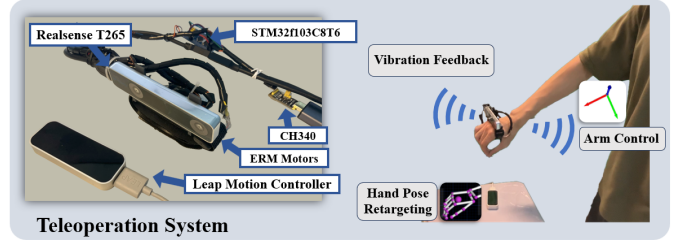


Fig. 2. The schematic diagram illustrates the self-developed hand-arm teleoperation system incorporating wrist force feedback for enhanced control accuracy and responsiveness.

## III. PROPOSED APPROACH

We design a diffusion-based visuo-proprioceptive imitation learning policy that accurately predicts the robot’s joint movements and contact forces using joint position and force feedback. An admittance-based low-level controller interpolates and tracks the force-position trajectories generated by the policy. This method is specifically tailored to optimize contact force management in tasks involving significant physical interactions, thereby minimizing the risk of damage while enhancing accuracy, efficiency, and stability. The frameworks for training and inference are illustrated in Fig. 3.

To evaluate the effectiveness of contact force control within visuo-proprioceptive imitation learning framework, we developed an hand-arm robotic system equipped with a wrist force sensor. Additionally, we designed a cost-effective force feedback teleoperation method tailored to this system. For the robotic hand, we opted for the Low-Cost, Efficient, and Anthropomorphic (LEAP) Hand, an open-source hardware by Shaw [38], which offers both affordability and ease of maintenance due to its 3D-printed parts and servo assembly. The servos in the LEAP Hand exhibit considerable robustness, allowing for nearly an hour of continuous operation during data collection without significant loss in joint output torque or overheating. By employing current-based position control in the servo joints, we can limit the output current for joint angle control, thereby achieving a degree of compliance in finger joint movement.

### A. Hand-Arm Teleoperation with Haptics

The complete system architecture and the operational workflow of the teleoperation system are illustrated in Fig. 2. The main components are as follows:

- A wrist spatial pose control module that estimates the 6-DoF spatial pose of the wearer’s wrist using the Intel RealSense Tracking Camera T265.
- A gesture detection and remapping module that estimates the spatial coordinates of the operator’s fingers using the Ultraleap Leap Motion Controller to map the human hand gestures to the multi-fingered robotic hand.
- A wrist contact force feedback module that uses a set of Eccentric Rotating Mass (ERM) vibration motors attached to the operator’s palm and driven by a microcontroller to provide feedback on the X-Y-Z axis force information read by the Force/Torque sensor on the robot’s wrist.

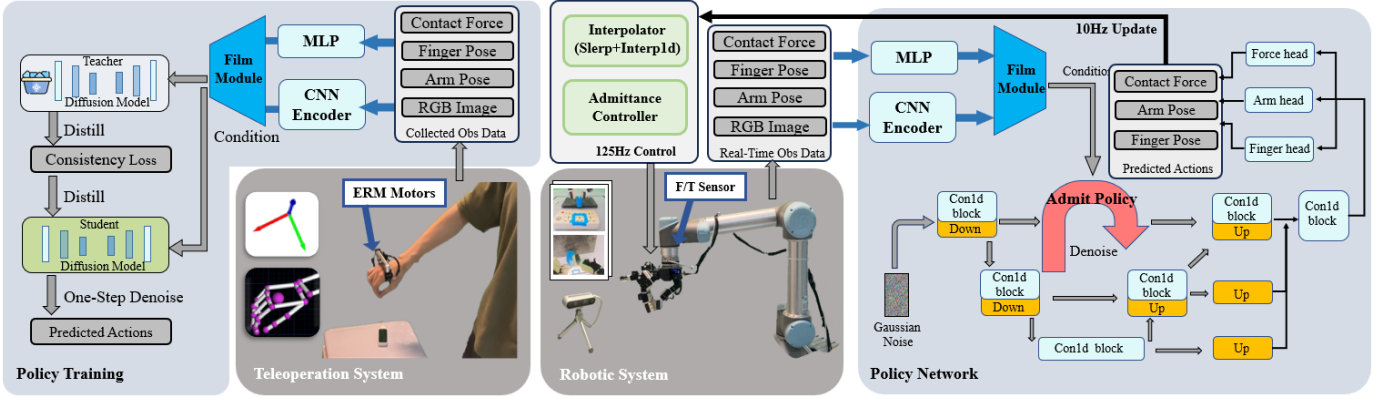


Fig. 3. Policy Training and Inference Framework. *Left*: The dataset is collected using our teleoperation system. And a teacher-student diffusion model is trained with consistency loss and distillation to refine policy predictions. *Middle*: The robotic system generates real-time multimodal data, including multiple RGB views, proprioceptive feedback, and force data. *Right*: The observations are sent to the policy network. Low-dimensional data are encoded using an MLP, and a multi-head mechanism is incorporated to accurately predict contact forces and joint angles.

The operator adjusts their movements in real-time based on vibration feedback from the ERM Vibration Motors, effectively controlling the contact force within an acceptable range to achieve force compliance during operation. Consequently, a compliance controller was not required to manage the robotic arm during teleoperation. In the gesture detection and remapping module, the Leap Motion Controller directly captures 21 spatial coordinate points to detect gestures. The process of kinematic retargeting, as outlined in [18], [19], involves remapping human hand gestures to the LEAP Hand by transforming joint angles into task-space vectors. An optimization problem is formulated to minimize the vector error within the task space, with the cost function defined as follows:

$$C(v_i^t, q_t) = \sum_{i=0}^N \left( |\alpha v_i^t - f_i(q_t)|^2 \right) + \beta |q_t - q_{t-1}|^2 \quad (1)$$

s.t.  $q_l \leq q_t \leq q_u$

where  $v_i^t$  is the keypoint vector of the human hand,  $f_i(q_t)$  is the keypoint vector calculated based on the joint angles  $q_t$  of the robotic hand, and  $\alpha$  and  $\beta$  are weight coefficients. The wrist spatial pose control module is a critical component of our hand-arm teleoperation system, enabling precise 6-DoF tracking of the wearer’s wrist. This module employs the Intel RealSense T265, which integrates dual fisheye cameras and an IMU to gather environmental and movement data. These data are fused via a Visual-Inertial Odometry program to provide accurate wrist position and pose information in 3D space. Following the approach in [19], we designed a simple glove using Velcro and 3D-printed parts to securely mount the T265 on the operator’s palm, facilitating high-precision control of the robot hand.

For wrist contact force feedback, we adopted a cost-effective method inspired by [39]. The system uses an stm32f103c8t6 microcontroller to generate Pulse Width Modulation (PWM) signals that control motor vibration intensity via an NPN Bipolar Junction Transistor transistor, based on force data from the wrist Force/Torque sensor. Contact forces between 0-20N are mapped linearly to vibration intensity, providing real-time feedback to the operator.

### B. Visuo-proprioceptive policy for Imitation Learning

Diffusion models have already found wide applications in image generation, so generating robotic actions in low-dimensional spaces is not a difficult task for diffusion models. Our imitation learning method, which combines vision and force, is based on a diffusion strategy. It uses this strategy to predict the future desired poses and forces, which are then utilized by an admittance controller to achieve compliant control. This mapping relationship can be expressed as:

$$f(I_{\text{global}}, I_{\text{local}}, s_{\text{proprio}}, F_{\text{current}}) \rightarrow (p_{\text{ee}}, q_{\text{finger}}, F_{\text{desired}}) \quad (2)$$

In this model, global and local camera images  $I_{\text{global}}, I_{\text{local}}$ , proprioceptive data  $s_{\text{proprio}}$ , and contact force measurements from a six-axis sensor  $F_{\text{current}}$  serve as input features. These inputs are linearly projected into a unified feature space via a FiLM module, which conditions the diffusion model to facilitate accurate noise prediction. Our noise prediction network is structured similarly to the diffusion policy. However, to mitigate information loss during the decoding phase and enhance the precision of action predictions, we extract features from multiple levels during the upsampling process, normalizing them to the same dimension and subsequently fusing them for final action prediction. To ensure that different types of action-related information do not interfere with each other, we employ multiple prediction heads, which also allow for a more precise formulation of the loss function.

While diffusion models are highly effective for generating multimodal robotic actions, the iterative multi-step denoising process can be computationally intensive, potentially compromising the compliance and dynamic performance of subsequent admittance control. Drawing inspiration from the Consistency Model (CM) [32], we introduce a consistency distillation approach into our visuo-proprioceptive imitation learning framework. By applying this method within the Probability Flow Ordinary Differential Equation (PFODE) framework, we train the model to produce consistent predictions across various points along the trajectory, ultimately enabling single-step denoising.

First, within the EDM [40] framework, a teacher model needs to be trained:

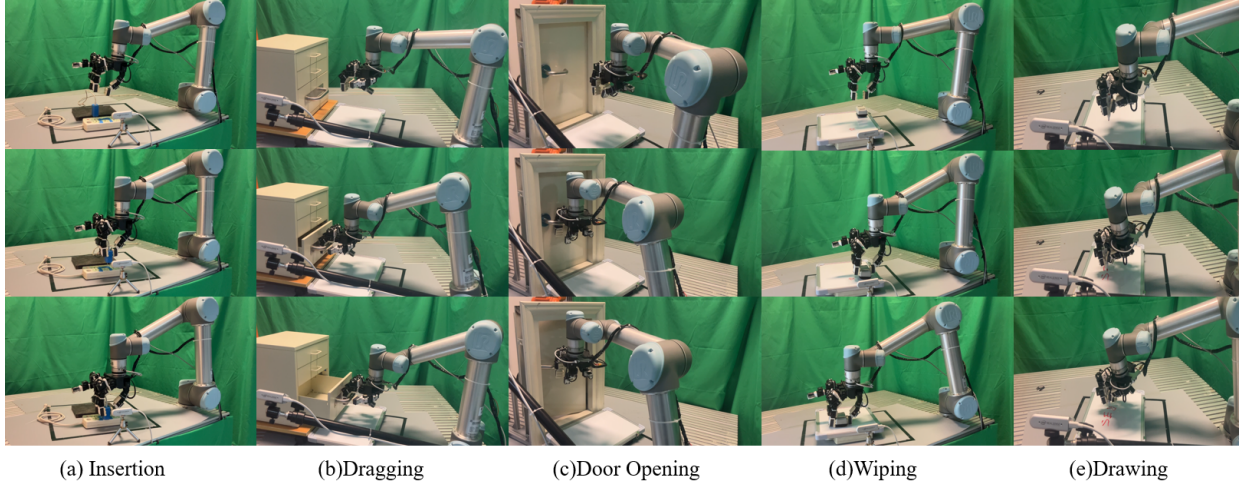


Fig. 4. Task Process Summary Diagram. We designed five contact-rich manipulation tasks to evaluate the effectiveness of the teleoperation system and the visuo-proprioceptive imitation learning algorithm, and compared them with other imitation learning algorithms. The success rate and contact force optimization results for different tasks are discussed later in this paper.

$$\frac{dA_t}{dt} = \frac{[A_t - \text{Teacher}_\theta(A_t, t; \text{obs})]}{t} \quad (3)$$

Its loss function is:

$$\mathcal{L}_{DSM} = \mathbb{E}_{\text{batch}} [\text{distance}(A_0, \text{Teacher}_\theta(A_t, t; \text{obs}))] \quad (4)$$

$$\text{distance}(x, y) = \sqrt{\|x - y\|^2 + c^2} - c \quad (5)$$

where  $c = 0.005 \times \sqrt{D}$ ,  $D$  is dimension of action. Given the PFODE trajectory of  $A_t$ , the initial  $A_0$  can be estimated, but at this time, the teacher model does not yet have the ability to predict  $A_0$  accurately in a single step. To achieve single-step denoising, the teacher model  $\text{Teacher}_\theta(A_t, t; \text{obs})$  needs to be distilled into the student model  $\text{Student}_\phi(A_t, t, t'; \text{obs})$ . The student can obtain  $A_{t'}$  at any earlier time from the action  $A_t$  at time  $t$ . The student model, initialized with the teacher model, is optimized with the goal of making predictions  $s$  at any two points  $u, v$  on the PFODE trajectory as close as possible:

$$\mathcal{L}_{CTM} = \mathbb{E}_{\text{batch}} [\text{distance}(\text{Student}_\phi(A_v, v, s; \text{obs}), \text{Student}_\phi(A_u, u, s; \text{obs}))] \quad (6)$$

where  $s < u < v$ ,  $A_u = \text{Teacher}_\theta(A_v, v, u; \text{obs})$ . Finally, the optimization formula for the student model is:

$$k_0 \mathcal{L}_{CTM} + k_1 \mathcal{L}_{DSM} \quad (7)$$

The trajectory points produced by the Diffusion Policy and Consistency Policy are updated at a frequency of 10Hz. However, to meet the demands of force control, which benefits from the highest possible control frequency, it is essential to interpolate the force-position trajectory points to achieve finer temporal resolution.

### C. Positional-based Interactive Force Control

Firstly, in robotic manipulation tasks, we define some common physical quantities. The pose of the robot's end-effector is represented by  $\mathcal{P}(t) = [R(t), p(t)] \in SE(3)$ , where  $R(t) \in SO(3)$  represents the rotation of the end-effector, and  $p(t) = [x(t), y(t), z(t)]^T \in \mathbb{R}^3$ .

The position of the end-effector in the base coordinate system is represented by  $p(t) \in \mathbb{R}^3$ . The interaction between the robot's end-effector and the external environment is described by the wrench  $\mathcal{W}(t) = [\mathcal{F}(t), \tau(t)] \in \mathbb{R}^6$ , where  $\mathcal{F}(t) = [f_x(t), f_y(t), f_z(t)]^T \in \mathbb{R}^3$  represents the force vector and  $\tau(t) \in \mathbb{R}^3$  represents the torque vector.

Secondly, referring to the impedance mathematical models presented in [41], we establish a dynamic model to control the interaction force between the robot and an unknown external environment when the robot needs to interact with such an environment:

$$M_d(\ddot{p}(t) - \ddot{p}_d(t)) + B_d(\dot{p}(t) - \dot{p}_d(t)) + K_d(p(t) - p_d(t)) = \mathcal{F}(t) - \mathcal{F}_d(t) \quad (8)$$

where  $M_d, B_d, K_d \in \mathbb{R}^{3 \times 3}$  denote the inertia, damping, and stiffness matrices in the contact dynamics between the robot end-effector and the environment, which regulate the contact behavior.  $\mathcal{F}$  and  $\mathcal{F}_d$  represent the feedback and desired force vectors of the robot end-effector.  $p$  and  $p_d$  represent the feedback and desired positions of the robot end-effector. Hence, the acceleration can be derived as:

$$\ddot{p}(t) = M_d^{-1}(\mathcal{F}(t) - \mathcal{F}_d(t) - B_d\dot{p}(t) - K_d(p(t) - p_d(t))) \quad (9)$$

Then we can update the acceleration and position according to the dynamics. The position will be used to control the robotic arm during inference:

$$\begin{aligned} \dot{p}(t + \Delta t) &= \dot{p}(t) + \ddot{p}(t) \cdot \Delta t \\ p(t + \Delta t) &= p(t) + \dot{p}(t) \cdot \Delta t \end{aligned} \quad (10)$$

We manually design the corresponding  $M_d$ ,  $B_d$ , and  $K_d$  parameters for different tasks to achieve better force-position tracking performance.

#### IV. EXPERIMENTS

##### A. Robot System Setup and Configuration

We have developed an integrated system for data collection and algorithm validation, which can be separated into the teleoperation system and the robotic system.

The robotic system features a 6-DoF collaborative robotic arm (UR5 cb3) equipped with a LEAP Hand at its end-effector. To facilitate interactive force control with feedback, an Opto-Force 6-Axis Force/Torque Sensor is mounted on the wrist of the robotic arm. Additionally, a RealSense D435i camera is installed on the workbench to provide visual feedback, with the optional addition of a USB Video Class (UVC) camera on the LEAP Hand’s palm for supplementary visual input.

The teleoperation system comprises an Intel RealSense T265 fisheye camera, an UltraLeap Leap Motion Controller, an stm32f103c8t6 microcontroller, and a set of ERM vibration motors. The entire robotic system is operated and controlled by a computer equipped with an Intel i9-12900K processor and an NVIDIA GeForce RTX 3090 GPU, which handles the training and inference of control policies.

##### B. Task Design and Implementation

We designed five manipulation tasks that involve high contact force; the experimental procedure is illustrated in Fig. 4.

1) *Insertion*: This task involves a peg-in-hole scenario. The robot begins by reaching for and grasping a charger plug, initially positioned randomly. It stabilizes the grasp with the index finger, middle finger, and thumb, then aligns the plug tip with a 2 cm hole, applying force along the Z-axis of the base coordinate system. In cases of misalignment, the robot adjusts by rotating the plug and applying corrective forces along the X and Y axes. Visual feedback is provided by both a global camera and a palm-mounted camera. The admittance controller parameters are  $M_d = 3$ ,  $B_d = 270$ , and  $K_d = 1540$ .

2) *Dragging*: In this task, the robot pulls a drawer, with a slightly randomized position but a fixed orientation along the X-axis. It inserts two fingers into the drawer handle and applies a consistent force along the X-axis. Only a global camera is used for visual guidance. The admittance controller parameters are  $M_d = 6$ ,  $B_d = 550$ , and  $K_d = 3000$ .

3) *Door Opening*: The robot opens a door by applying significant forces (20–40 N) across all three axes. It grasps the handle with the index and middle fingers and applies a downward force with the palm to rotate the handle, then pushes along the positive X-axis to open the door. A global camera provides visual feedback. The admittance controller parameters are  $M_d = 10$ ,  $B_d = 900$ , and  $K_d = 5000$ .

4) *Wiping*: This task requires the robot to wipe a whiteboard. The robot grasps a randomly placed eraser with three fingers, moves to the marked area, and applies forces along the Z and X axes to clean. Both a global camera and a palm-mounted camera are used. The admittance controller parameters are  $M_d = 5$ ,  $B_d = 300$ , and  $K_d = 2000$ .

5) *Drawing*: This task involves drawing on a whiteboard. The robot grasps a marker and maintains a consistent contact force along the Z-axis while following a predefined trajectory. Visual feedback is provided by both a global camera and a palm-mounted camera. The admittance controller parameters are  $M_d = 3$ ,  $B_d = 270$ , and  $K_d = 1540$ .

We collected 50 demonstration trajectories for each task and performed post-processing on the data within these trajectories. The rotation vector representing the robot’s end-effector pose was converted to the Rotation6D [42] format, and a first-order low-pass filter was applied to the contact force data. Each task was trained for 400 epochs using the 50 demonstrations, which took approximately 8 hours. Extending the training duration in the diffusion policy can lead to better convergence. On the physical system, the inference time for the Diffusion Policy (DP) is about 100 ms, while the inference time for the Consistency Model (CM) is around 7 ms.

#### V. RESULTS

Before collecting demonstration trajectories, we tested our teleoperation system on the Telekinesis Benchmark task, which evaluates the performance of multi-finger robotic teleoperation.

TABLE I  
TELEOPERATION SYSTEMS EVALUATION RESULTS IN TELEKINESIS BENCHMARK.

Task	System	Success	Time (s)
Pickup Box Object	Spacemouse+Leap	17/20	20.7
	AnyTeleop	20/20	16.2
	Ours w/o Haptic	19/20	14.5
	<b>Ours</b>	<b>20/20</b>	<b>11.1</b>
Pickup Fabric Toy	Spacemouse+Leap	12/20	21.3
	AnyTeleop	17/20	17.0
	Ours w/o Haptic	18/20	15.8
	<b>Ours</b>	<b>18/20</b>	<b>13.7</b>
Box Rotation	Spacemouse+Leap	15/20	24.5
	AnyTeleop	18/20	18.5
	Ours w/o Haptic	19/20	17.0
	<b>Ours</b>	<b>20/20</b>	<b>13.9</b>
Open Drawer	Spacemouse+Leap	12/20	21.5
	AnyTeleop	16/20	20.2
	Ours w/o Haptic	18/20	16.0
	<b>Ours</b>	<b>20/20</b>	<b>13.3</b>
Two Cup Stacking	Spacemouse+Leap	14/20	24.5
	AnyTeleop	14/20	20.0
	Ours w/o Haptic	16/20	18.5
	<b>Ours</b>	<b>18/20</b>	<b>15.8</b>

Each method was tested 20 times per task. Our approach exhibited superior precision and speed over monocular vision-based systems (e.g. Telekinesis, AnyTeleop), while also offering a better user experience than non-wearable devices (e.g. SpaceMouse). On average, our method reduced task time by 8.94 seconds compared to the Spacemouse+Leap system, and by 4.82 seconds compared to AnyTeleop. Additionally, it increased the success rate by 26% over Spacemouse+Leap, and by 11% over AnyTeleop.

TABLE II  
SUCCESS RATES OF REAL EXPERIMENTS ON FIVE DIFFERENT TASKS.

Method	Insertion	Opening	Dragging	Wiping	Drawing	Average
Diffusion policy	60%	70%	80%	70%	20%	60%
Consistency policy	70%	75%	80%	75%	25%	70%
Admit policy w/o Force	75%	80%	85%	85%	40%	73%
Admit policy (Ours)	<b>90%</b>	<b>95%</b>	<b>95%</b>	<b>90%</b>	<b>45%</b>	<b>83%</b>

We evaluated the success rates of four different methods across five tasks, with each method undergoing twenty trials. The success rates obtained from these experiments are detailed in Table II, where our proposed policy consistently outperformed the other methods across all tasks. In tasks with stringent contact force control requirements, such as Peg-Insertion and Wiping, our method demonstrated up to a 30% improvement in success rate compared to approaches lacking force control. While methods without force control could still achieve relatively high success rates, our experimental analysis indicated that these approaches exhibited greater fluctuations and oscillations in contact force during task execution.

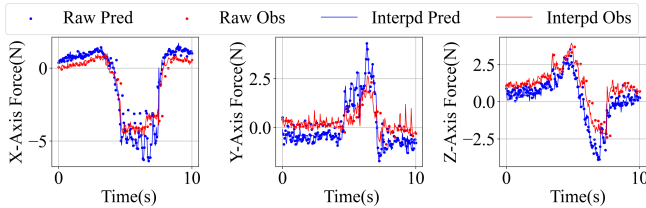


Fig. 5. Force control interpolation and tracking performance on different axes in dragging task.

Our visuo-proprioceptive policy estimates a consistent future force-position trajectory points, with each point spaced 0.1 seconds apart. The admittance controller takes these trajectory points as desired inputs, applying one-dimensional linear interpolation (Interp1d) for the target positions and contact forces, and spherical linear interpolation (Slerp) for the target rotations, to generate a densely sampled trajectory curve.

Throughout the entire process, the contact force is maintained within a stable and low range. Quantitative analysis of the data reveals that, when pulling the drawer in the negative X-axis direction, a constant contact force of approximately -4.5 N is exerted along the negative X-axis in the world coordinate frame. The Root Mean Square Error (RMSE) of the force tracking is around 0.8 N, which is sufficient to enable the robot to perform the task in a stable and compliant manner.

To illustrate the interpolation process and the tracking of the desired force trajectory, we collected experimental data from the drawer-opening task, as shown in Fig. 5. It is observed that the policy's estimation of the contact force modality exhibits some fluctuations due to the inherent variability in proprioceptive contact force measurements.

We compared the Diffusion Policy and Consistency Policy with the Admit Policy incorporating force feedback input but without force control, as well as the Admit Policy with force feedback and force control, during the door-opening task. The result can be seen in Fig. 6. The comparison focused on the mean contact force and the standard deviation of force

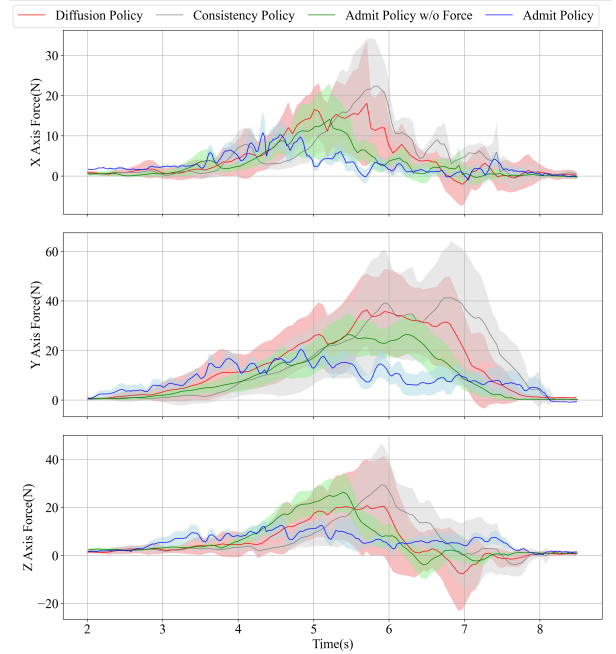


Fig. 6. Comparison of Mean and Standard Deviation of Forces During the Door-Opening Task Across Four Different Methods

variation along the X, Y, and Z axes of the base coordinate system.

The Diffusion and Consistency Policies showed similar mean contact forces, but the Consistency Policy had more stable trajectory transitions. The distilled Consistency Policy, with fewer parameters, exhibited slight fluctuations in trajectories. Under positional control, it produced larger contact force fluctuations compared to the Diffusion Policy. Across all axes, the Admit Policy reduced mean force by up to 53.92% and force variation by up to 76.51%. Without force feedback control, it estimated forces and, with the admittance controller, reduced contact force variation by 49.21%.

## VI. CONCLUSIONS

In this paper, we propose a novel visuo-proprioceptive imitation learning method to enhance contact-rich manipulation tasks, successfully applying it to several complex robotic operations. By integrating visual perception with force feedback, our approach improves operational accuracy and stability while enhancing compliant control during task execution.

The cost-effective hand-arm teleoperation system we developed supports data collection and strategy validation for future complex contact-rich tasks. Experimental results show that the system efficiently collects high-quality demonstration data and achieves robust control in contact-rich environments.

Moreover, by incorporating force control into the imitation learning strategy, we significantly improved the force-position tracking performance during real-world operations, reducing errors and minimizing the risk of damage. Our method has exhibited outstanding performance across multiple experimental tasks, demonstrating its practicality and advantages in addressing complex force-interaction scenarios.

In future work, we plan to further optimize the inference speed of the imitation learning strategy and explore its application in more complex task scenarios to further validate the broad applicability of the method.

## REFERENCES

- [1] M. Suomalainen, Y. Karayiannidis, and V. Kyrki, "A survey of robot manipulation in contact," *Robotics and Autonomous Systems*, vol. 156, p. 104224, 2022.
- [2] C. C. Beltran-Hernandez, D. Petit, I. G. Ramirez-Alpizar, and K. Harada, "Variable compliance control for robotic peg-in-hole assembly: A deep-reinforcement-learning approach," *Applied Sciences*, vol. 10, no. 19, p. 6923, 2020.
- [3] B. Siciliano, "Springer handbook of robotics," *Springer-Verlag google schola*, vol. 2, pp. 15–35, 2008.
- [4] S. Scherzinger, A. Roennau, and R. Dillmann, "Learning human-inspired force strategies for robotic assembly," in *2023 IEEE 19th International Conference on Automation Science and Engineering (CASE)*, pp. 1–8, IEEE, 2023.
- [5] T. Z. Zhao, V. Kumar, S. Levine, and C. Finn, "Learning fine-grained bimanual manipulation with low-cost hardware," *arXiv preprint arXiv:2304.13705*, 2023.
- [6] C. Wang, H. Shi, W. Wang, R. Zhang, L. Fei-Fei, and C. K. Liu, "Dex-cap: Scalable and portable mocap data collection system for dexterous manipulation," *arXiv preprint arXiv:2403.07788*, 2024.
- [7] Y. Ze, G. Zhang, K. Zhang, C. Hu, M. Wang, and H. Xu, "3d diffusion policy," *arXiv preprint arXiv:2403.03954*, 2024.
- [8] K. Darvish, L. Penco, J. Ramos, R. Cisneros, J. Pratt, E. Yoshida, S. Ivaldi, and D. Pucci, "Teleoperation of humanoid robots: A survey," *IEEE Transactions on Robotics*, vol. 39, no. 3, pp. 1706–1727, 2023.
- [9] C. Coppola, G. Solak, and L. Jamone, "An affordable system for the teleoperation of dexterous robotic hands using leap motion hand tracking and vibrotactile feedback," *2022 31st IEEE International Conference on Robot and Human Interactive Communication (RO-MAN)*, pp. 920–926, 2022.
- [10] S. Li, X. Ma, H. Liang, M. Görner, P. Ruppel, B. Fang, F. Sun, and J. Zhang, "Vision-based teleoperation of shadow dexterous hand using end-to-end deep neural network," in *2019 International Conference on Robotics and Automation (ICRA)*, pp. 416–422, IEEE, 2019.
- [11] S. P. Arunachalam, S. Silwal, B. Evans, and L. Pinto, "Dexterous imitation made easy: A learning-based framework for efficient dexterous manipulation," in *2023 IEEE International Conference on Robotics and Automation (ICRA)*, pp. 5954–5961, IEEE, 2023.
- [12] Y. Qin, Y.-H. Wu, S. Liu, H. Jiang, R. Yang, Y. Fu, and X. Wang, "Dexmv: Imitation learning for dexterous manipulation from human videos," in *European Conference on Computer Vision*, pp. 570–587, Springer, 2022.
- [13] Y. Qin, H. Su, and X. Wang, "From one hand to multiple hands: Imitation learning for dexterous manipulation from single-camera teleoperation," *IEEE Robotics and Automation Letters*, vol. 7, no. 4, pp. 10873–10881, 2022.
- [14] K. Shaw, S. Bahl, and D. Pathak, "Videodex: Learning dexterity from internet videos," in *Conference on Robot Learning*, pp. 654–665, PMLR, 2023.
- [15] T. Zhang, Z. McCarthy, O. Jow, D. Lee, X. Chen, K. Goldberg, and P. Abbeel, "Deep imitation learning for complex manipulation tasks from virtual reality teleoperation," in *2018 IEEE International Conference on Robotics and Automation (ICRA)*, pp. 5628–5635, IEEE, 2018.
- [16] Y.-P. Su, X.-Q. Chen, T. Zhou, C. Pretty, and G. Chase, "Mixed-reality-enhanced human-robot interaction with an imitation-based mapping approach for intuitive teleoperation of a robotic arm-hand system," *Applied Sciences*, vol. 12, no. 9, p. 4740, 2022.
- [17] S. Li, J. Jiang, P. Ruppel, H. Liang, X. Ma, N. Hendrich, F. Sun, and J. Zhang, "A mobile robot hand-arm teleoperation system by vision and imu," in *2020 IEEE/RSJ International Conference on Intelligent Robots and Systems (IROS)*, pp. 10900–10906, 2020.
- [18] Y. Qin, W. Yang, B. Huang, K. Van Wyk, H. Su, X. Wang, Y.-W. Chao, and D. Fox, "Anyteleop: A general vision-based dexterous robot arm-hand teleoperation system," *arXiv preprint arXiv:2307.04577*, 2023.
- [19] A. Handa, K. Van Wyk, W. Yang, J. Liang, Y.-W. Chao, Q. Wan, S. Birchfield, N. Ratliff, and D. Fox, "Dexipilot: Vision-based teleoperation of dexterous robotic hand-arm system," in *2020 IEEE International Conference on Robotics and Automation (ICRA)*, pp. 9164–9170, IEEE, 2020.
- [20] Z. Fu, Q. Zhao, Q. Wu, G. Wetzstein, and C. Finn, "Humanplus: Humanoid shadowing and imitation from humans," *arXiv preprint arXiv:2406.10454*, 2024.
- [21] P. Wu, Y. Shentu, Z. Yi, X. Lin, and P. Abbeel, "Gello: A general, low-cost, and intuitive teleoperation framework for robot manipulators," *arXiv preprint arXiv:2309.13037*, 2023.
- [22] C. Chi, Z. Xu, C. Pan, E. Cousineau, B. Burchfiel, S. Feng, R. Tedrake, and S. Song, "Universal manipulation interface: In-the-wild robot teaching without in-the-wild robots," *arXiv preprint arXiv:2402.10329*, 2024.
- [23] C. Wang, L. Fan, J. Sun, R. Zhang, L. Fei-Fei, D. Xu, Y. Zhu, and A. Anandkumar, "Mimicplay: Long-horizon imitation learning by watching human play," *arXiv preprint arXiv:2302.12422*, 2023.
- [24] C. Chi, S. Feng, Y. Du, Z. Xu, E. Cousineau, B. Burchfiel, and S. Song, "Diffusion policy: Visuomotor policy learning via action diffusion," *arXiv preprint arXiv:2303.04137*, 2023.
- [25] A. Sridhar, D. Shah, C. Glossop, and S. Levine, "Nomad: Goal masked diffusion policies for navigation and exploration," in *2024 IEEE International Conference on Robotics and Automation (ICRA)*, pp. 63–70, IEEE, 2024.
- [26] A. Iyer, Z. Peng, Y. Dai, I. Guzey, S. Haldar, S. Chintala, and L. Pinto, "Open teach: A versatile teleoperation system for robotic manipulation," *arXiv preprint arXiv:2403.07870*, 2024.
- [27] S. Haldar, J. Pari, A. Rai, and L. Pinto, "Teach a robot to fish: Versatile imitation from one minute of demonstrations," *arXiv preprint arXiv:2303.01497*, 2023.
- [28] E. Jang, A. Irpan, M. Khansari, D. Kappler, F. Ebert, C. Lynch, S. Levine, and C. Finn, "Bc-z: Zero-shot task generalization with robotic imitation learning," in *Conference on Robot Learning*, pp. 991–1002, PMLR, 2022.
- [29] A. Brohan, N. Brown, J. Carbajal, Y. Chebotar, X. Chen, K. Choromanski, T. Ding, D. Driess, A. Dubey, C. Finn, *et al.*, "Rt-2: Vision-language-action models transfer web knowledge to robotic control," *arXiv preprint arXiv:2307.15818*, 2023.
- [30] S. Haldar, Z. Peng, and L. Pinto, "Baku: An efficient transformer for multi-task policy learning," *arXiv preprint arXiv:2406.07539*, 2024.
- [31] T. Yang, Y. Jing, H. Wu, J. Xu, K. Sima, G. Chen, Q. Sima, and T. Kong, "Moma-force: Visual-force imitation for real-world mobile manipulation," in *2023 IEEE/RSJ International Conference on Intelligent Robots and Systems (IROS)*, pp. 6847–6852, IEEE, 2023.
- [32] A. Prasad, K. Lin, J. Wu, L. Zhou, and J. Bohg, "Consistency policy: Accelerated visuomotor policies via consistency distillation," *arXiv preprint arXiv:2405.07503*, 2024.
- [33] T. Ren, Y. Dong, D. Wu, and K. Chen, "Learning-based variable compliance control for robotic assembly," *Journal of Mechanisms and Robotics*, vol. 10, no. 6, p. 061008, 2018.
- [34] Q. Liu, Z. Ji, W. Xu, Z. Liu, B. Yao, and Z. Zhou, "Knowledge-guided robot learning on compliance control for robotic assembly task with predictive model," *Expert Systems with Applications*, vol. 234, p. 121037, 2023.
- [35] N. Hogan, "Impedance control: An approach to manipulation: Part ii—implementation," in *1984 American Control Conference*, 1984.
- [36] C. C. Beltran-Hernandez, D. Petit, I. G. Ramirez-Alpizar, T. Nishi, S. Kikuchi, T. Matsubara, and K. Harada, "Learning force control for contact-rich manipulation tasks with rigid position-controlled robots," *IEEE Robotics and Automation Letters*, vol. 5, no. 4, pp. 5709–5716, 2020.
- [37] T. Kamijo, C. C. Beltran-Hernandez, and M. Hamaya, "Learning variable compliance control from a few demonstrations for bimanual robot with haptic feedback teleoperation system," *arXiv preprint arXiv:2406.14990*, 2024.
- [38] K. Shaw, A. Agarwal, and D. Pathak, "Leap hand: Low-cost, efficient, and anthropomorphic hand for robot learning," *arXiv preprint arXiv:2309.06440*, 2023.
- [39] R. Ding, Y. Qin, J. Zhu, C. Jia, S. Yang, R. Yang, X. Qi, and X. Wang, "Bunny-visionpro: Real-time bimanual dexterous teleoperation for imitation learning," *arXiv preprint arXiv:2407.03162*, 2024.
- [40] T. Karras, M. Aittala, T. Aila, and S. Laine, "Elucidating the design space of diffusion-based generative models," *Advances in neural information processing systems*, vol. 35, pp. 26565–26577, 2022.
- [41] H. Liu, L. Wang, and F. Wang, "Fuzzy force control of constrained robot manipulators based on impedance model in an unknown environment," *Frontiers of Mechanical Engineering in China*, vol. 2, pp. 168–174, 2007.
- [42] Y. Zhou, C. Barnes, J. Lu, J. Yang, and H. Li, "On the continuity of rotation representations in neural networks," in *Proceedings of the IEEE/CVF conference on computer vision and pattern recognition*, pp. 5745–5753, 2019.